Mechanism of the hardening process for a hydroxyapatite cement

Changsheng Liu,* Wei Shen, and Yanfang Gu
Institute of Technical Chemical Physics, East China University of Science and Technology, P.O. Box 258, Shanghai 200237, Peoples Republic of China

The dynamics for the hydraulic process of calcium phosphate cement (CPC) were investigated by X-ray diffraction quantitative analysis. The results show that the hardening process of CPC is initially controlled by the dissolution of reactants in a 4-h period and subsequently by diffusion through the product layer of hydroxyapatite (HAP) around the grains. The compressive strength rises approximately linearly with the increase of the extent of conversion in a 4-h period, and a maximum compressive strength of about 51 MPa, which is superior to those reported by the references, is obtained in 4 h. Then the compressive strength drops a little with an increase in the extent of conversion. The final product of setting reaction is acicular HAP crystal. Crystal seed not only reduces the setting time but also drops the compressive strength. The variation of pH in CPC slurry from 7.5 to 10.5 reveals that the control step of the dissolution process in the hardening process is the dissolution of dicalcium phosphate anhydrous and the presence of crystal seed will reduce the supersaturation to produce HAP. © 1997 John Wiley & Sons, Inc.

INTRODUCTION

A calcium phosphate cement (CPC) which is capable of self-setting under ambient conditions has recently been reported.[1,2] CPC is a mixture of a basic calcium phosphate, tetracalcium phosphate [(TECP), $Ca_4(PO_4)_2O$], with an acidic calcium phosphate, dicalcium phosphate anhydrous [(DCPA), $CaHPO_4$]. When CPC is mixed with a hardening solution, it becomes a slurry that can be shaped to any contour and set to harden under physiological conditions to form hydroxyapatite (HAP). The setting reaction is:

$$Ca_4(PO_4)_2O + CaHPO_4 \xrightarrow[H_2O]{} Ca_5(PO_4)_3OH$$

This process is very different from the formation of HAP ceramic which is created by sintering, where HAP powder formed by precipitation is heated to 800–1200°C. The CPC has an advantage over HAP ceramic for its contour adaptability, while both are highly compatible with the tissues,[3–6] because the final products are HAP, which is similar to the mineral component of mammalian hard tissue.

The hardening process of CPC is complex and involves the dissolution of solid particles in liquid, precipitation of HAP from solution, and reaction and diffusion on the particle surface. Under ideal conditions,[2] continuing dissolution of the reactants supplies calcium and phosphate ions to the solution, while HAP formation depletes these ions. This process drives the solution composition to an invariant point which is the intersection of the solubility curves for these two reactants. The pH is about 7.8,[7] but this process is affected by many parameters, such as the component of the solid phase, the particle sizes of TECP and DCPA, presence of HAP seed and properties, aqueous liquid, etc. There have been few investigations reported concerning the mechanism of CPC hydration. Brown et al.[8,9] studied calcium-deficient HAP (Ca/P = 1.5) formation by isothermal conduction calorimetry and variations in solution chemistry. The first step was the formation of HAP, but details were not given. Fukase et al.[10] investigated the setting reaction of CPC, but the mechanism of this process was not proposed and the compressive strength was low. The purposes of this article were to investigate the mechanism of the hardening process, and to make clear the relationship among kinetics, microstructure development, and variations of pH in slurry. All of these are fundamental physicochemical properties for further research and application.

*To whom correspondence should be addressed.

Journal of Biomedical Materials Research, Vol. 35, 75–80 (1997)

CCC 0021-9304/97/010075-06

EXPERIMENTAL PROCEDURES

Hydroxyapatite was prepared by a precipitation method.[11] DCPA was prepared by heating $CaHPO_4 \cdot 2H_2O$ at 120°C for about 6 h, for dehydration. TECP was prepared by heating an equimolar mixture of DCPA and $CaCO_3$ at 1500°C for 24 h[12] and then was ground in a pulverizer to obtain a suitable particle size. The DCPA was ground in anhydrous ethanol followed by drying at 80°C. The specific surface area (SSA) of the TECP was 0.732 m^2/g, while the SSAs of the DCPA used in different examples were 9.76, 6.90, and 2.82 m^2/g, respectively, (ASAP2400; Micrometritics Co.). These phase-pure components were then combined according to the desired composition for the cement.

The solid phase consists of an equimolar mixture of TECP and DCPA. In some samples, a 3% low crystallinity HAP of 10–20 nm was present for the purpose of increasing the rate of setting reaction. No other additive was included, since it was not expected to produce any significant effect on the composition of the cement. To prepare a specimen, 0.6 g of CPC powder (the SSA of DCPA used was 6.9 m^2/g) was mixed with 0.15 mL of the aqueous solution so that the powder-to-liquid ratio (P/L) was 4.0 (wt./wt.), which was the optimum value determined in a previous study. The solid and liquid were stirred with a stainless-steel spatula to form a paste in 1 min, and then the paste was loaded into a stainless-steel mold (6 × 12 mm) with periodic packing by means of a stainless-steel rod (5.6 mm in diameter). The force applied to the rod during packing was 2 kg, corresponding to a pressure of 8.2 kg/cm^2, which is the same as the method reported by Fukase et al.[10] The specimen was removed and put into a glass tube (8 × 20 mm), and then the glass tube was sealed with film and stored in a 37°C, 100% humidity box for 0.5, 1, 2, 3, 4, 24, or 48 h. After predetermined intervals, the hardened specimens were measured for compressive strengths; five specimens were used for each selected interval.

Compressive strength measurement

The compressive strength of the specimen was measured with the loading rate of test of 1 mm/min on a universal testing machine (AG-2000A, Shimadzu Autograph, Shimadzu Co., Ltd., Japan).

X-ray diffraction analysis

After the compressive strength measurement, portions of the crushed piece of specimen were immediately placed in a bottle containing acetone (100%), cooled to −80°C, and freeze-dried to stop the setting reaction at the selected interval, and the freeze-dried samples were ground to fine powders. Then the extent of conversion of the samples at specific periods was determined by the quantitative analysis method of x-ray diffraction with sodium chloride as an internal standard (Model P.MAX/γ B; Rigaku Co). The relative peak areas of TECP at 29.2° and 29.8°, 2θ of HAP at 25.9°, and of NaCl at 45.4° were determined to estimate the extent of conversion. These were the only major peaks of the reactions free of overlapping. To eliminate the influence of machine error and the trace residual of reactions in the results of a 24-h specimen, the standard curve should be made before determining the specimens, and all diffraction measurements should be finished at the unit operating time.

The specimen in the 48-h period was taken as a standard material for HAP, since the conversion reaction was stopped basically within 48 h from the previous experiments. Samples with different combinations of HAP, TECP, and DCPA were obtained and then mixed with NaCl (9:1 wt./wt.) to determinate the peak intensities. The peak area ratios of HAP and TECP to NaCl were plotted to the percentages of HAP and TECP in the samples, respectively, shown in Figure 1.

Scanning electron microscopy (SEM)

Some freeze-dried samples at various intervals after compressive strength measurement were collected and examined by SEM (S-250MKII; Cambridge Co.) to observe the development of microstructure.

pH measurement

The pH of the slurry prepared by mixing 3 g equimolar mixture of TECP-DCPA with 1.5 mL of deionic water was measured by pH meters in a 4-h period, since the compressive strength was up to the maximum value and the slurry was setting hard within the period, as described later. Different combinations of the presence and absence of crystal seed and variations in the SSA of DCPA were made to explore the hardening process.

RESULTS AND DISCUSSION

Dynamics for hydraulic process

The specimens obtained at various intervals were analyzed; the results showed that the final product

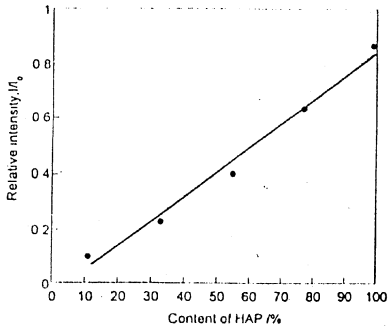

Figure 1. Standard curve for HAP.

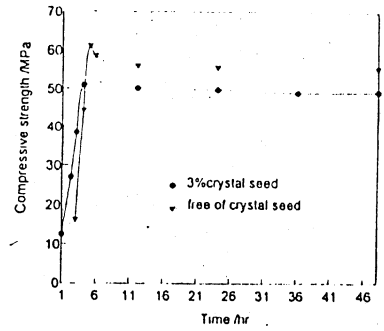

Figure 3. Variation of compressive strengths with time in CPC specimens.

was HAP, but there was an amount of residual TECP in the 48-h samples. Since it is difficult to eliminate the influence of these residuals on the results, the extent of producing HAP was taken as the conversion ratio. The results showed (Fig. 2) that the reactant rate (slope of tangent of the curve) was large at the earlier stage and then became slower and slower with time after 4 h. The conversion ratio was approximately linear with time in the 4-h period.

According to the traditional mechanisms for cement hydration,[13] there are three kinds of dynamic models: controlled by surface dissolution of solid particle

$$G_I = r_0 [1 - (1 - \alpha)^{1/3}] = k_I t$$

controlled by nucleation and crystal growth

$$G_N = [-\ln(1 - \alpha)]^{1/3} = k_N t$$

controlled by diffusion through product layer

$$G_D = r_0^2 [1 - (1 - \alpha)^{1/3}]^2 = k_D t$$

where r_0 is the initial radius of the particle.

k_N, k_I, and k_D were calculated with experimental data, respectively, and then the hydration models were calculated using the coefficient above and comparing it with the experiment. The results showed that no models coincided ideally with experimental data. Only the composite model which was controlled by surface dissolution of reactant particles at an earlier stage and by diffusion through the HAP layer at later periods was identical with the experimental data. Whether DCPA or TECP was the control step for the dissolution process could not be determined at this time.

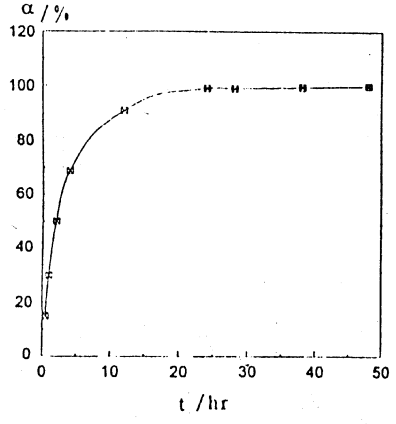

Figure 2. Relationship between conversion ratio of HAP and reactant time in CPC.

Compressive strength

Figure 3 indicates the compressive strengths of the CPC specimens at various intervals and the effects of the presence or absence of crystal seed on compressive strengths.

At the initial 4-h stage, the compressive strength of CPC specimens rose with time approximately linearly. The maximum value was obtained in 4 h with the presence of 3% HAP as the crystal seed compared with that obtained within 5 h free of crystal seed in CPC specimens. There was a slight decline in compressive strength at the later period. The results also showed that the compressive strengths of CPC speci-

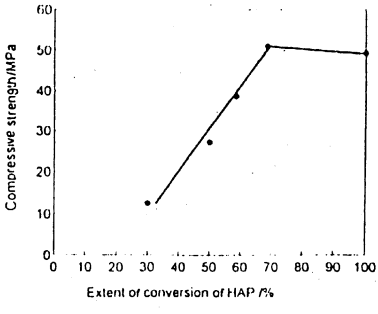

Figure 4. Correlation between compressive strength and the extent of the conversion.

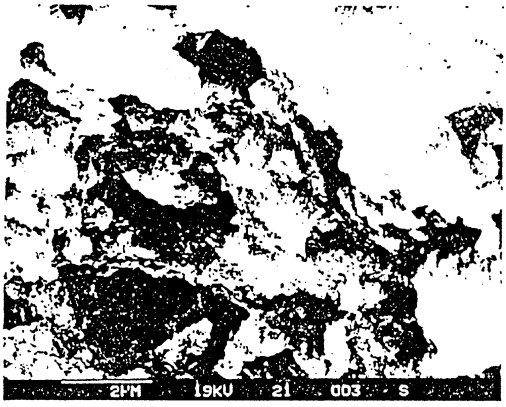

Figure 5. SEM micrograph of specimen obtained at 17 min. Bar represents 2 μm.

mens were approximately linear with the extent of the conversion, α (R = 0.987) (Fig. 4). However, when the extent of conversion, α, was >69%, the compressive strengths decreased with the increase of α.

The results reported by Fukase et al.[10] also revealed the same phenomenon that the compressive strength at 24 h was lower than that at 4 h, but the author did not mention or discuss it. The mechanism of the hardening process discussed above may explain this phenomenon. Hydration is controlled by the dissolution of reactant particles in the 4-h period, and since the rate of dissolution is proportional to the surface area of the particles which was basically constant in CPC specimens in the earlier stage, the precipitation rate of HAP is linear with time. HAP was formed among the reactant particles which would enhance the joint of solids, or around the particles which would reduce the distance of grains. All of these are beneficial to a rise in compressive strength. Therefore, the increases in the compressive strengths were linear with both time and the extent of conversion. However, when a shell of HAP was formed around the reactants, which was found by Brown et al.,[9] the rate of HAP formation was controlled by the transport of water and ions through such a shell and decreased with an increase of the thick HAP shell. Since the densities of DCPA and HAP were different, 2.31 and 3.16 g/cm^3, respectively, the hydration of the residual DCPA engulfed by the shell to HAP would lead to an internal force which would be harmful to the compressive strength. Thus, the compressive strengths decreased with the process of hydration at the later stage.

Figure 3 shows that the maximum compressive strength of specimens free of crystal seed was 61 MPA obtained 5 h after mixing, while 51 MPa was obtained after 4 h in specimens containing 3% of crystal seed. The setting times of specimens with the presence and absence of crystal seed were 20 and 180 min, respectively. They indicate that the presence of crystal seed not only reduced the setting time but also dropped the compressive strength. This result was confirmed by another study[14] and was different from the data reported by Fukase et al.[10] and Chow.[15] Fukase et al. and Chow thought that HAP included in the mixture reduced setting time but increased the compressive strength, but the causes of these results were not mentioned. The mechanism of crystal seed affecting the hardening process was investigated further in Hu et al.[14]

The compressive strength for the 24-h specimens is 50 MPa; while in another study, the compressive strength of 71 MPa in a 24-h specimen was obtained with the presence of crystal seed and a combination of the different SSAs of DCPA and TECP (unpublished). All these were significantly higher than the values of 36 MPa reported by Fukase et al.,[10] 34 MPa reported by Brown and Chow,[2] and 21 MPa reported by Doi et al.[16]

Development of microstructure of CPC

The specimens at 17 min (beginning to set), 70 min, and 48 h after mixing were examined by SEM. Micrograph of specimen obtained at 17 min showed (Fig. 5) the morphology of the grains and the spatial relationship between DCPA and TECP. No acicular material representing HAP was found. However, at 70 min, some amorphous materials among the grains were found in the specimen (Fig. 6), which consisted of small petal-like or needlelike crystals revealed by higher-magnification micrographs. These crystals were responsible for the adherence of grains resulting in hardening. In the 24-h sample (Fig. 7), the amount and form of the intergrain materials became larger

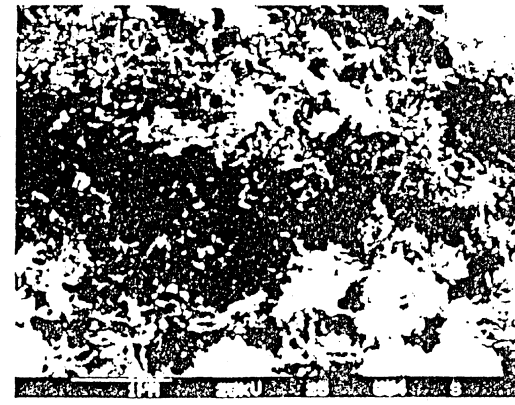

Figure 6. SEM micrograph of specimen obtained at 70 min. Bar represents 1 μm.

Figure 7. Microstructure of 24-h sample by SEM. Bar represents 4 μm.

than before, and the outlines of particles were less apparent. The grains were adjacent to each other or linked by large needlelike or flat crystals.

The high-density materials occupied originally by reactant particles were wrinkled and consisted of small acicular crystals (Fig. 8). The different morphologies of crystals were formed in different ways: the needlelike crystal intergrains were formed by dissolution control at the earlier stage; the wrinkled crystals were formed by diffusion control at the later stage.

Variation of pH in CPC slurry

The variation of pH with time in CPC slurry is shown in Figure 9.

The difference of Figure 9(a) from Figure 9(c) is the presence of 5% crystal seed, while Figure 9(c) is free of crystal seed. In Figure 9(c), the variation of pH is very gentle and is always maintained at 8.6–8.8 after 10 min. With absence of crystal seed in Figure 9(a), the pH is up to 10.6 after 15 min and then down to 9.0 after 60 min, which indicates that more basic TECP was solved before the crystal took place. Therefore, it was deduced that the crystal did not occur until the supersaturation was up to a high value by the solution of DCPA and TECP in the absence of crystal seed. At a range of high pH value, the solubility of the acidic DCPA increased while the solubility of the basic TECP decreased, which resulted in the decrease of pH. Steady-state was finally achieved.

Figure 9(a) and (b) are absent of crystal seed, but the SSA of DCPA is bigger in Figure 9(b) than in Figure 9(a), and so is the dissolved rate of DCPA, which would lead to a decrease of pH. The pH in Figure 9(b) is lower than Figure 9(a) at the same time. Figure 9(c) and (d) were similar to Figure 9(a) and (b) except for the presence of crystal seed, and a similar conclusion was also obtained.

Therefore, we conclude that the dissolution process is controlled by the SSA of DCPA which would greatly affect the hardening process, and the presence of crystal seed would reduce the supersaturation to produce HAP.

Brown[7] reported that when DCPA and TECP form an invariant point in $Ca(OH)_2$—H_3PO_4—H_2O ternary system; the pH at this invariant point is about 7.8. All of the steady-state pH values obtained were higher than this value. Thus, although steady-state pH conditions were reached and maintained, an invariant condition was not achieved.

CONCLUSION

The hardening process of CPC is the process of HAP formation. The rate of HAP formation is initially controlled by dissolution of reactants within 4 h and subsequently by diffusion through the product layer of HAP around the particles. In a 4-h period, both compressive strength and extent of conversion are approximately linear with reactant time and correlate with one another. The maximum compressive strength is obtained at about 51 MPa at 4 h, which is superior to those reported by the literature. The compressive strength has a little drop with an increase of the extent of conversion after it is larger than 70%. The presence of crystal seed not only reduces the setting time but also drops the compressive strength, which is affirmed by another study but is inconsistent with Chow's conclusion. The highest compressive strength of samples free of crystal seed is about 61 MPa. The final product of the setting reaction is acicular or needlelike crystal HAP. The pH in CPC slurry varies from 7.5 to 10.6 according to the different combina-

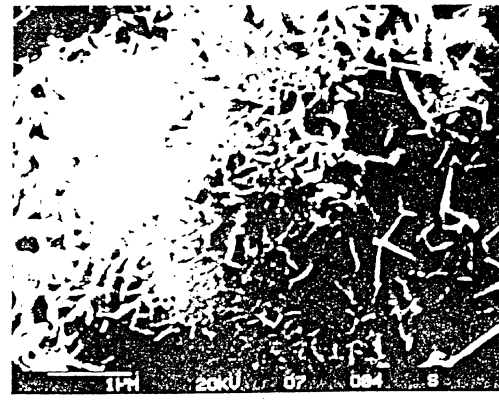

Figure 8. Detail of Figure 7 showing morphologies of hydroxyapatite. Bar represents 1 μm.

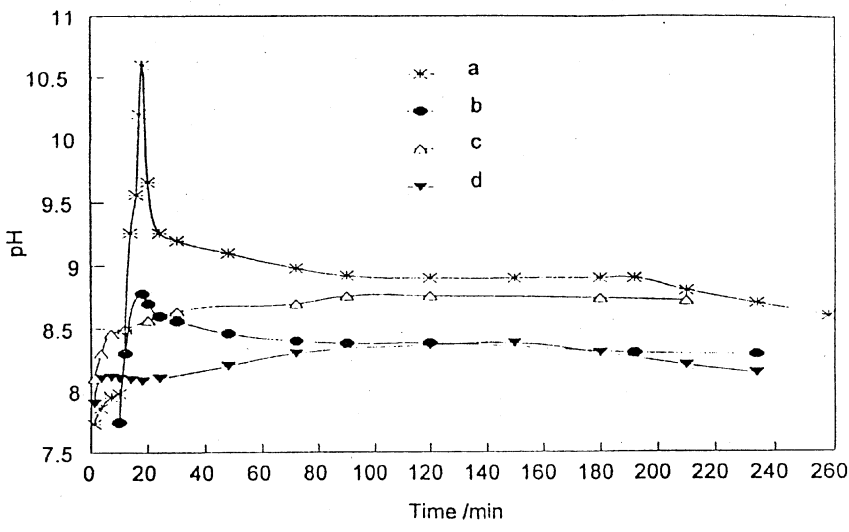

Figure 9. Variation of pH in the slurry with time after mixing DCPA and TECP with water. The SSA of TECP is 0.732 m^2/g. (a) SSA of DCPA is 2.82 m^2/g, free of crystal seed. (b) SSA of DCPA is 9.87 m^2/g, free of crystal seed. (c) SSA of DCPA is 2.82 m^2/g; 5% crystal seed presented. (d) SSA of DCPA is 9.87 m^2/g; 5% crystal seed presented.

tions of SSA of DCPA, and whether or not the crystal seed exists. The results revealed that the control step of the dissolution process is the dissolution of DCPA, and the presence of crystal seed would reduce the supersaturation to produce HAP.

This work is supported by the National Natural Science Foundation, China.

References

1. W. E. Brown and L. C. Chow, "A new calcium phosphate setting cement," *J. Dent. Res.*, 63, 672 (1983).
2. W. E. Brown and L. C. Chow, "A new calcium phosphate, water-setting cement," in *Cements Research Progress*, P. W. Brow (ed.), American Ceramic Society, Westerville, Ohio, 1986, pp. 352–379.
3. P. D. Costantino, C. D. Friedman, K. Jones, L. C. Chow, and G. A. Sisson, "Experimental hydroxyapatite cement cranioplasty," *Plastic Reconstr. Surg.*, 90, 174–185 (1992).
4. S. E. Gruninger, C. Siew, L. C. Chow, A. O. Brown, and W. E. Brown, "Evaluation of the biocompatibility of a new calcium phosphate setting cement," *J. Dent. Res.*, 63, 200 (1984).
5. A. A. Chohayeb, L. C. Chow, and P. Tsaknis, "Evaluation of calcium phosphate as root canal sealer-filler material," *J. Endodont.*, 13, 384–387 (1987).
6. A. Sugawara, L. C. Chow, S. Takagi, and H. Chohayeb, "In vitro evaluation of the sealing ability of a calcium phosphate cement when used as a root canal sealer-filler," *J. Endodont.*, 16, 162–165 (1990).
7. W. E. Brown, "Solubilities of phosphates and other sparingly soluble compounds," in *Environmental Phosphorous Handbook*, Z. J. Griffith, A. Beeton, J. M. Spencer, and D. T. Mitchell (eds.), Wiley, New York, 1973, pp. 203–239.
8. P. W. Brown and M. Fulmer, "Kinetics of hydroxyapatite formation at low temperature," *J. Am. Ceram. Soc.*, 74, 934–940 (1991).
9. P. W. Brown, N. Hocker, and S. Hoyle, "Variations in solution chemistry during the low-temperature formation of hydroxyapatite," *J. Am. Ceram. Soc.*, 74, 1848–1854 (1991).
10. Y. Fukase, E. D. Eanes, S. Takag, L. C. Chow, and W. E. Brown, "Setting reactions and compressive strengths of calcium phosphate cement," *J. Dent. Res.*, 69, 1852–1856 (1990).
11. E. C. Moreno, T. M. Gregory, and W. E. Brown, "Preparation and solubility of hydroxyapatite," *J. Res. Nat. Bureau Stand. U.S.*, 72A, 773–782 (1968).
12. W. E. Brown and E. F. Epstein, "Crystallography of tetracalcium phosphate," *J. Res. Nat. Bureau Stand. U.S.*, 69A, 547–551 (1965).
13. A. Bezjak and I. Jelenic, "On the determination of rate constants for hydration processes in cement pastes," *Cem. Concr. Res.*, 10, 553–563 (1980).
14. L. M. Hu, C. S. Liu, and W. Shen, "Study on the calcium phosphate cement for bone reconstruction," IUMRS-ICA-95, Seoul.
15. L. C. Chow, "Development of self-setting calcium phosphate cements," *Centennial Memorial Issue of the Ceramic Society of Japan*, 99, 954–964 (1991).
16. Y. Doi, Y. Takezawa, S. Shibata, N. Wakamatsu, H. Kamemizu, T. Goto, M. Ijima, Y. Morikawi, K. Uno, F. Kubo, and Y. Haeuchi, "Self-setting apatite cement. I. Physicochemical properties," *J. Jpn. Soc. Dent. Mater. Dev.*, 6, 53–58 (1987).

Received December 26, 1995
Accepted May 2, 1996